

Poly- ϵ -caprolactone based nanoparticles for delivery of genistein in melanoma treatment

Juliana Palma Abriata¹, Marcela Tavares Luiz¹, Juliana Santos Rosa Viegas¹,
Fernando Fumagalli², Shaiani Maria Gilde Melo¹, Flavio da Silva Emery¹,
Juliana Maldonado Marchetti¹, Fabiana Testa Moura de Carvalho Vicentini¹

¹School of Pharmaceutical Sciences of Ribeirão Preto, University of São Paulo, São Paulo, Brazil, ²Health Sciences Center (CCS), Federal University of Santa Maria (UFSM), Santa Maria, Rio Grande do Sul, Brazil

We developed poly- ϵ -caprolactone (PCL)-based nanoparticles containing D- α -tocopherol polyethylene glycol-1000 succinate (TPGS) or Poloxamer 407 as stabilizers to efficiently encapsulate genistein (GN). Two formulations, referred to as PNTPGS and PNPOL, were prepared using nanoprecipitation. They were characterized by size and PDI distribution, zeta potential, nanoparticle tracking analysis (NTA), GN association (AE%), infrared spectroscopy (FT-IR), and differential scanning calorimetry (DSC). PNTPGS-GN exhibited a particle size of 141.2 nm, a PDI of 0.189, a zeta potential of -32.9 mV, and an AE% of 77.95%. PNPOL-GN had a size of 146.3 nm, a better PDI than PNTPGS-GN (0.150), a less negative zeta potential (-21.0 mV), and an AE% of 68.73%. Thermal and spectrometric analyses indicated that no new compounds were formed, and there was no incompatibility detected in the formulations. Cellular studies revealed that Poloxamer 407 conferred less toxicity to PCL nanoparticles. However, the percentage of uptake decreased compared to the use of TPGS, which exhibited almost 80% cellular uptake. This study contributes to the investigation of stabilizers capable of conferring stability to PCL nanoparticles efficiently encapsulating GN. Thus, the PCL nanoparticle proposed here is an innovative nanomedicine for melanoma therapy and represents a strong candidate for specific pre-clinical and *in vivo* studies.

Keywords: Genistein. Polymer-based Nanoparticles. HPLC-UV. D- α -tocopherol polyethylene glycol-1000 succinate. Nanoparticles stabilizers.

INTRODUCTION

Genistein (GN) is a natural molecule in *Genista tinctoria* L. and widely distributed in leguminous plants, including seeds, fruits, and vegetables. It is an isoflavone known as 5,7-dihydroxy-3-(4-hydroxyphenyl) chromen-4-one, belonging to the group of aglycones. Isoflavones can exhibit estrogen-like functions in mammals, acting either as estrogen agonists or antagonists by interacting with estrogen receptors. This is particularly due to their carbons 4 and 7 on phenol rings, which have a similar chemical structure to

hormones, easily binding to both estrogen receptors (Goh *et al.*, 2022; Sharifi-Rad *et al.*, 2021).

Recent studies have suggested that GN has the potential to reduce the risk of tumor formation (Farina *et al.*, 2006), by inhibiting various tyrosine protein kinases, topoisomerase II, S6 kinase activities, and promoting the inhibition of tumor cell proliferation, differentiation, and apoptosis induction. GN shows promise in reducing mortality from solid tumors and metastases, making it a candidate for treatment of various cancer types (Hewitt, 2003; Kuzumaki, Kobayashi, Ishikawa, 1998; Pavese, Farmer, Bergan, 2010).

Despite the potential for GN in cancer treatment, its effects on gene expression and toxicity are not fully understood. High doses of GN have been shown to cause

*Correspondence: F. T. M. C. Vicentini. Departamento de Ciências Farmacêuticas. Faculdade de Ciências Farmacêuticas de Ribeirão Preto. Universidade de São Paulo. Avenida Professor Doutor Zeferino Vaz, s/n, 14040903, Ribeirão Preto, SP, Brazil. Phone: (55)16 33154257. E-mail: fabtesta@fcrp.usp.br. ORCID: <https://orcid.org/0000-0002-0842-9130>

side effects that affect cellular pathways (Singh *et al.*, 2014). Additionally, its low aqueous solubility reduces its bioavailability, often necessitating solubilization in dimethyl sulfoxide (DMSO) for *in vitro* and *in vivo* studies (Singh *et al.*, 2014). However, DMSO is a dose-dependently cytotoxic solvent that can interact with cellular metabolism and membranes, leading to cellular apoptosis in both tumor and normal cells (Da Violante *et al.*, 2002). This raises concerns about the suitability of DMSO for GN application.

Various approaches have been explored to mitigate GN toxicity, reduce the use of toxic solvents, enhance treatment specificity and prevent melanoma cell progression (Cui *et al.*, 2017). Nanocarriers have gained attention for delivering chemotherapeutic agents due to their potential advantages, including reduced side effects, improved therapeutic efficacy, ease of administration, and increased patient compliance (Li, Wallace, 2008). Among nanocarriers, polymeric nanoparticles offer significant potential to minimize pharmacotherapeutic challenges by sustaining drug release, extending residence time in bloodstream, reducing required doses and administration frequency, achieving high drug encapsulation efficiency, protecting against degradation, and reducing irritant potential due to their polymeric coating (Crucho, Barros, 2017; Mora-Huertas *et al.*, 2012).

In the development of drug delivery systems like nanoparticles, evaluating their physicochemical properties is essential, as they depend on the proportions of each component. Ionic compounds, in particular, can modify the surface charge, influencing nanoparticle interactions with cells and the biological environment. Stabilizers play a critical role in ensuring the stability of nanoparticles. However, the charge and organic group configuration of stabilizers can lead to interactions with cell membranes that affect charge flow, potentially impacting cell viability (Giuliano *et al.*, 2018a).

In this study, we aimed to develop poly- ϵ -caprolactone (PCL)-based nanoparticles using two different stabilizers, D- α -tocopherol polyethylene glycol-1000 succinate (TPGS) and Poloxamer 407. Both PCL-based systems, each containing one of these stabilizers, were characterized and evaluated for their ability to form nanoparticles with appropriate characteristics in terms of particle size, charge,

and low polydispersity. High GN encapsulation was also a key requirement. Cellular studies were conducted to assess the effectiveness of these nanoparticles in optimizing GN release to cells while maintaining controlled toxicity and promoting high uptake.

MATERIAL AND METHODS

Material

Genistein (GN) was acquired from API Chem Technology (China). Poly- ϵ -caprolactone (PCL) with a molecular weight of 14,000 g mol⁻¹, D- α -tocopherol polyethylene glycol-1000 succinate (TPGS), and Poloxamer 407 (Pol) were obtained from Sigma-Aldrich (USA). High-performance liquid chromatography (HPLC) grade acetonitrile was purchased from Baker (USA), and acetone (P.A.) used for all formulations was sourced from Synth (Brazil).

HPLC-UV method validation for genistein quantification

Genistein (GN) was quantified following the method of De Carvalho Zampieri *et al.* (2013). A high-performance liquid chromatograph coupled with a UV detector (Thermo Scientific® Dionex UltiMate 3000) and an RP-18 column (LiChroCART® 250-4 LiChrospher® 100 RP-18 - 5 μ m) were employed under the following chromatography conditions: a UV detector with a wavelength of 270 nm, an isocratic mobile phase consisting of acetonitrile: water acidified with orthophosphoric acid (pH 3.0) at a 70:30 v/v ratio, a flow rate of 1.0 mL min⁻¹, an injection sample volume of 20 μ L, and an oven compartment temperature maintained at 25 °C throughout the analysis. Analytical concentrations of GN were prepared at 0.5, 1.0, 2.5, 5.0, 7.5, and 10.0 μ g mL⁻¹ from a 1000 μ g mL⁻¹ GN stock solution. The HPLC-UV method was validated according to the International Conference on Harmonization (ICH) document Q2 (R1), including the assessment of selectivity, linearity, intermediate precision, repeatability, inter- and intra-assay accuracy, and detection and quantification limits. The precision

and accuracy were determined in the intermediate precision (inter-assay) and repeatability (intra-assay) of GN at concentrations of 0.5, 5.0, and 10.0 $\mu\text{g mL}^{-1}$, with acceptable coefficients of variation (CV) values of < 5% (Mora-Huertas *et al.*, 2012).

Nanoparticle preparation

Poly- ϵ -caprolactone (PCL)-based nanoparticles were prepared using the nanoprecipitation technique. In this process, the organic phase (OP), consisting of polymer (PCL) and drug (GN) (28.79 mg and 1.7 mg, respectively), was solubilized in acetone, and subjected to ultrasound for 30 minutes. The aqueous phase (AP), containing the stabilizer TPGS (0.4%, w/v) or Poloxamer 407 (0.5%, w/v) in 7.58 mL of 30 mM phosphate buffer (pH 7.4), received the OP under stirring. The resulting suspension was stirred at 600 rpm for 24 hours at 25 °C until complete solvent evaporation.

Physicochemical characterization

Dynamic light scattering (DLS) and Zeta Potential

The particle size and polydispersity index (PDI) were determined using a light scattering analyzer (Zetasizer Malvern Nano ZS, USA) at a controlled temperature of 25 °C and a detection angle of 173°. Each formulation was diluted in ultrapure water (1:25). Zeta potential was determined through electrophoretic mobility (Zetasizer Malvern Nano ZS, USA), with each formulation diluted in ultrapure water (1:50).

Nanoparticle tracking analysis (NTA)

NTA was conducted using a Nano Sight LM20 instrument (Nano Sight, United Kingdom) with NTA 2.0 Analytical software (Nano Sight, UK). Measurements were performed after dilution (1:500) of the nanoparticles, both with and without GN, in particle-free ultrapure water. The diluted nanoparticles were introduced into the sample holder using a sterile syringe until completely filled (0.5 mL). Analyses were performed using a diode

laser beam ($\lambda = 635 \text{ nm}$). Size measurements were conducted in triplicate, with data expressed as the mean \pm standard deviation.

Association efficiency (AE%) of GN

AE% was determined using Amicon® 10 KDa devices, with the ultrafiltrate quantified by HPLC, as previously described. The GN ultrafiltrate content corresponded to the non-encapsulated GN. Encapsulated GN and drug loading (DL) capability were determined using Equation 1 and Equation 2, respectively.

$$\%EE = \frac{(\text{Total GN} - \text{nonencapsulated GN}) \times 100}{\text{Total GN}} \quad (1)$$

$$\%DL = \frac{(\mu\text{g GN encapsulated into PN}) \times 100}{\mu\text{g total of PN (GN+PCL+stabilizer)}} \quad (2)$$

Differential scanning calorimetry (DSC)

DSC analysis (Thermal Analysis Workstation, Perkin Elmer, USA) was performed for GN, lyophilized nanoparticles with and without GN (5 mg each). The samples were placed in an aluminum crucible under a nitrogen atmosphere (3 Kgf/cm²) and subjected to analysis. An empty aluminum crucible served as a reference. The analysis involved heating at a rate of 10°C. min⁻¹ from 30°C to 350°C. Data were analyzed using TAS-Thermal Analysis Workstation software.

Infrared Spectroscopy - Fourier Transform (FT-IR)

FTIR analysis (Shimadzu IR Prestige-21 equipment) was conducted for GN and lyophilized nanoparticles with or without GN. Each sample was analyzed in KBr pellets, with a resolution of 2 cm⁻¹, within the range of 4000 to 400 cm⁻¹.

Cell viability studies

Cell viability studies were performed using Resazurin (25 $\mu\text{g mL}^{-1}$) as a viability indicator. Normal fibroblasts (3T3) and melanoma cells (Sk-mel-103) were

seeded at 10,000 cells per well in 96-well plates and cultured at 37 °C in a 5% CO₂ atmosphere. Following adhesion, cells were exposed to various treatments, including free GN, PNTPGS, PNPoI controls, and formulations containing GN. Cell viabilities were assessed after 72 hours of exposure.

Uptake studies

PCL-BODIPY was used to prepare nanoparticles to monitor their uptake via flow cytometry (FACS Canto I). Initially, 25,000 cells were seeded per well in 12-well plates and then incubated with nanoparticles at concentrations of 20 µM (1.5×10^{10} nanoparticles per mL) and 100 µM (3.3×10^{11} nanoparticles per mL) for 24 hours. Propidium Iodide (50 µg/mL) was used to assess cell viability. The analysis was conducted using excitation at 488 nm and emission at 530 nm for BODIPY, and at 488 nm and 670 nm for propidium iodide. Results were expressed as percentages (%).

Statistical analysis

The experimental data were analyzed using Two-way ANOVA and Tukey's test with a 95% confidence level. At least three replicates were used for each statistical analysis. This statistical analysis was performed using GraphPad Prism 8.

RESULTS AND DISCUSSION

HPLC method validation for genistein (GN) quantification

The development of the genistein quantification method was performed according to De Carvalho Zampieri *et al.* (2013) with adaptations. Initially, we utilized an ACN: water mobile phase (pH 4.5) at a ratio of 50:50 (v/v), which yielded a GN peak at 75 µg/mL with a trailing tail. Subsequently, we explored different mobile phase compositions and pH conditions, including ACN: water (pH 4.5) at 55:45 (v/v), ACN: water (pH 3.0) at 55:45 (v/v), ACN: water (pH 3.0) at 65:35 (v/v), ACN: water (pH 3.0) at 60:40 (v/v), and ACN: water (pH 3.0) at 70:30 (v/v). Additionally, it was investigated the impact of methanol by testing ACN: methanol: water (pH 3.0) at 55:20:25 (v/v) and ACN: methanol: water (pH 3.0) at 55:10:35 (v/v). Although some conditions still exhibited tailing, ACN: water (pH 3.0) at 70:30 (v/v) produced a chromatographic peak with excellent resolution, devoid of tailing, and a retention time of 2.5 minutes.

With optimized chromatography conditions, we proceeded to validate the method. The first parameter assessed was selectivity. To determine potential interference, it was individually injected the components of each formulation into the HPLC (Figure 1). We did not observe any chromatographic peaks at the GN retention time (approximately 2.5 minutes), suggesting that the nanoparticles' components do not interfere with GN analysis. Consequently, the method is selective for quantifying genistein encapsulated within polymeric nanoparticles.

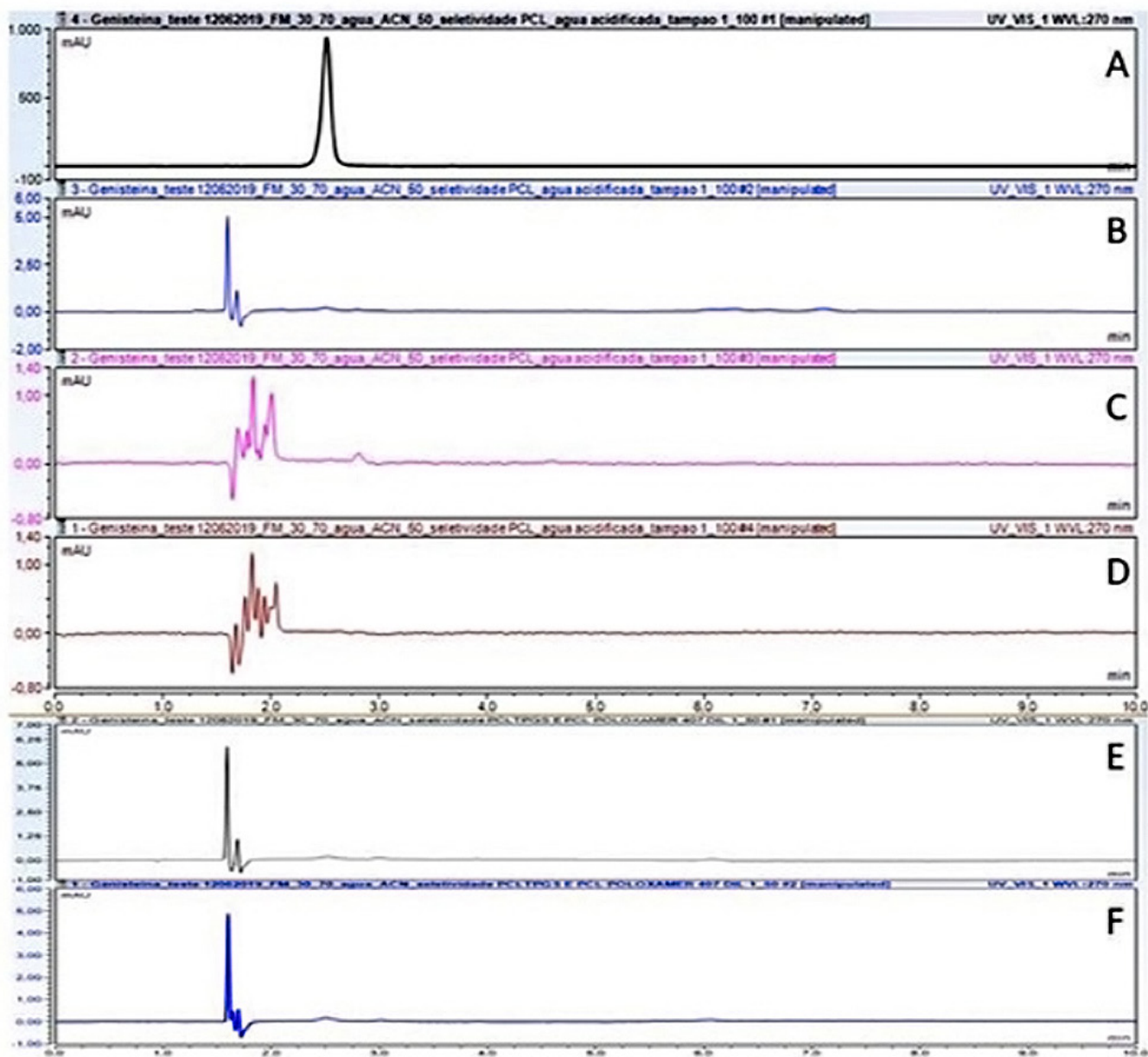


FIGURE 1 – Chromatograms demonstrating the selectivity of formulation components at 1:50 dilution, (A) 50 $\mu\text{g.mL}^{-1}$ genistein, (B) water acidified with orthophosphoric acid pH 3.0, (C) 30 μM phosphate buffer, (D) PCL-TPGS Solution on ACN and (E) PCL-Poloxamer 407 Solution on CAN.

The second parameter examined was linearity, assessing the relationship between analyte concentration and response. Three analytical curves were constructed spanning the range of 0.5 to 10 $\mu\text{g mL}^{-1}$, evaluating the coefficient of variation (CV%) and the linear correlation coefficient (r^2). The responses exhibited direct proportionality to sample concentration within the specified range, with r^2 values exceeding 0.9999,

establishing a linear range of 0.5 to 10 $\mu\text{g mL}^{-1}$. The HPLC method demonstrated a linear correlation between GN concentrations and chromatograph areas, expressed by the regression equation: $y = 1.9242x - 0.2298$.

Precision is a crucial aspect of HPLC methods, ensuring consistent results close to the theoretical value across repetitions (Mora-Huertas *et al.*, 2012). The proposed GN quantification method exhibited precision,

as indicated by CV values below 5% for both intermediate precision and repeatability (Table I). Furthermore, the method demonstrated accuracy, with experimental results (expressed as % recovery) aligning with the theoretical concentrations. The experimentally determined limits of detection and quantification were 0.1 $\mu\text{g. mL}^{-1}$ and 0.5 $\mu\text{g. mL}^{-1}$, respectively.

The results establish the HPLC-UV method as a reliable means for GN quantification, validated through selectivity, linearity, accuracy, and precision, in accordance with recommendations from the International Conference on Harmonization of Technical Requirements for Registration of Pharmaceuticals for Human Use (Mora-Huertas *et al.*, 2012).

TABLE I - Intermediate precision and repeatability, and intra-assay and inter-assay accuracy of the analytical method validated for the quantification of GN by HPLC-UV (n = 3)

Precision		
Concentration ($\mu\text{g.mL}^{-1}$)	Repeatability (CV%)	Intermediate precision (CV%)
0.5	0.37	1.08
5.0	0.21	2.47
10.0	0.70	0.54
Accuracy		
Concentration ($\mu\text{g.mL}^{-1}$)	Intra-assay recovery (%)	Inter-assay recovery (%)
0.5	100.22 \pm 0.018	101.43 \pm 3.77
5.0	98.85 \pm 0.022	99.36 \pm 0.45
10.0	100.10 \pm 0.008	100.20 \pm 0.085

The results are the mean \pm SD of three experiments.

Nanoparticle characterization

Nanoprecipitation is a well-established technique known for its simplicity, minimal use of toxic solvents, and independence from high shear stress, sonication, or elevated temperatures. Initially developed by Fessi and colleagues (1989) for hydrophobic drugs and water-miscible solvents like ethanol and acetone, among others

(De Carvalho Zampieri *et al.*, 2013; Giuliano *et al.*, 2018a). The technique requires the inclusion of a stabilizer to prevent particle aggregation and enhance system stability. Among various stabilizers, TPGS, a water-soluble vitamin E derivative, and PEG, both FDA-approved for various routes of administration (ICH 2005), have gained widespread use due to their ability to improve drug encapsulation efficiency and nanoparticle internalization. TPGS, in particular, demonstrates synergistic growth inhibition when combined with other antitumor drugs by inducing apoptosis in tumor cells. Its hydrophilic coating minimizes plasma protein adsorption onto nanoparticle surfaces, reducing clearance by the liver and spleen and facilitating intravenous administration route (BRASIL, 2017). Despite the common use of TPGS, poloxamer 407, a copolymer aiding hydrophobic molecule solubilization, has found application as a stabilizer in nano-systems. Notably, poloxamer 407 exhibits lower toxicity compared to other stabilizers (Almeida *et al.*, 2012; Giuliano *et al.*, 2018a, 2018b).

Stringent control of particle size is essential since the smallest blood capillaries typically have diameters ranging from 4 to 7 μm . Nanometric particles help prevent capillary occlusion and facilitate drug distribution (Fessi *et al.*, 1989; Legrand *et al.*, 2007). To avoid phagocytosis by macrophages and ensure an extended circulation time in the bloodstream, nanoparticles should be less than 200 nm. This size range is especially beneficial for tumor applications since nanoparticles within it tend to accumulate in solid tumors, thanks to the Enhanced Permeability and Retention (EPR) effect (Nordström 2011).

Consequently, the average diameter of nanoparticles significantly influences their circulation time in the bloodstream, propensity for leakage, particle direction, immunogenicity, internalization, and degradation. Additionally, particle size plays a crucial role in determining how nanoparticles interact with and adhere to blood vessels, which, in turn, can impact their clearance (Yan *et al.*, 2007).

Characterization of PCL nanoparticles is summarized in Table II. Both TPGS and poloxamer 407-stabilized nanoparticles exhibited sizes within the range of 110 - 150 nm, with polydispersity indices (PDIs) below 0.2, indicating a monomodal distribution. Notably,

the zeta potential for PNTPGS was approximately -30 mV, while PNPOL displayed neutrality ($|\leq 30|$ mV), consistent with the non-ionic nature of Poloxamers.

Nano-tracking analysis (NTA) results aligned with dynamic light scattering (DLS) data. NTA, equipped with a charge-coupled device, allows for real-time determination of particle sizes individually (Filipe, Hawe, Jiskoot, 2010). For PNTPGS and PNTPGS-GN formulations, modal particle sizes were 131.6 ± 1.2 nm and 135.3 ± 3.4 nm, respectively. In contrast, PNPOL and PNPOL-GN formulations exhibited modal sizes of 143.1 ± 0.7 nm and 155.4 ± 1.0 nm, respectively. NTA also provided particle concentration per milliliter, ranging from 10^{11} to 10^{12} particles for all formulations, a critical characterization for predicting dose-response in *in vitro* and *in vivo* tests (Gross *et al.*, 2016).

Determination of GN encapsulation indicated that both stabilizers assisted in its encapsulation, with TPGS showing higher efficiency. After assessing particle size, concentration, zeta potential, and encapsulation efficiency, we conducted thermal and spectrometric analyses to check

for any interactions, incompatibilities, or degradation. As per Zhang *et al.* (2015), GN typically exhibits an endothermic peak at 301.7°C , which we observed in our study at around 303.7°C . Danciu *et al.* (2015) also reported similar findings, with GN displaying an endothermic peak at 303°C , followed by an exothermic peak at 307°C , signifying chemical decomposition. In our DSC analysis of PNTPGS-GN (Figure 2-A) and PNPOL-GN (Figure 2-B) formulations, it was not detected any additional peaks, confirming that no new composites formed due to degradation, chemical reactions, or incompatibilities.

In the FT-IR analysis of GN (Figure 2-C), we observed distinct bands characteristic of GN, including absorption bands related to the stretching vibrations of phenolic-OH groups (3411 and 3109 cm^{-1}), C = O (1649 cm^{-1}), C = aromatic C (ranging from 1563 to 1494 cm^{-1}), and CO connections (1287 cm^{-1}) (Pool *et al.*, 2018). However, in the nanoparticles containing GN, these characteristic GN bands were no longer detectable. This suggests that GN was successfully encapsulated within the nanoparticles.

TABLE II - Summary of PCL-based nanoparticles characteristics containing or not GN

PCL-based nanoparticle	Size (nm)	PDI	Zeta Potential (mV)	AE%	%DL	Nanoparticles/ mL
PNTPGS control	129.1	0.089	-31.3	-	-	$4.79 \times 10^{11} \pm 1.88 \times 10^{11}$
PNTPGS-GN	141.2	0.189	-32.9	77.95	3.70	$4.85 \times 10^{12} \pm 2.81 \times 10^{10}$
PNPOL control	110.1	0.126	-17.1	-	-	$2.2 \times 10^{12} \pm 5.5 \times 10^{11}$
PNPOL-GN	146.3	0.150	-21.0	68.73	1.50	$4.2 \times 10^{12} \pm 2.5 \times 10^{11}$

AE% association efficiency, %DL drug loading.

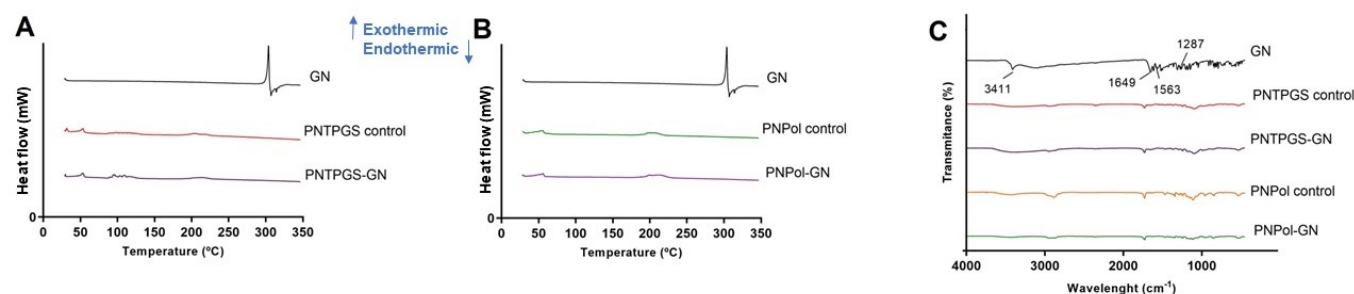


FIGURE 2 – DSC analysis of GN and the PCL nanoparticles with TPGS (PNTPGS) control and containing GN (A) and poloxamer 407 (PNPOL) control and containing GN (B), as well as FT-IR analysis of them (C). The heat involved was in ΔG .

Cell viability and uptake studies

Melanoma cells, specifically Skmel-103, exhibited a high sensitivity to GN, as expected due to their higher metabolic activity compared to 3T3 cells, which are non-malignant. This heightened sensitivity to GN in melanoma cells has been previously reported in various studies (Danciu *et al.*, 2015; Dobrzynska, Napierala, Florek, 2020; Ji *et al.*, 2012; Rauth, Kichina, Green, 1997; Tyagi, Song, De, 2019; Venza *et al.*, 2018).

In the context of the two systems developed (Figure 3) involving PCL-based nanoparticles with either TPGS or poloxamer 407, the nanoparticles incorporating TPGS demonstrated greater cytotoxicity compared to those containing poloxamer 407. In 3T3 cells, free GN exhibited a 50% reduction in viability only at a concentration of 75 nM. However, in melanoma cells, the impact of GN on viability was notable, with a decline observed at concentrations as low as 20 nM, reaching 50% viability reduction at 50 nM.

In comparison between PNTPGS control and PNPOL control, PNTPGS was more cytotoxic. Moreover, when GN was added to both PNTPGS and PNPOL, the cytotoxic effect was intensified. Notably, PNPOL-GN exhibited significantly lower cytotoxicity than PNTPGS-GN. For instance, at a concentration of 20 nM (Figure 3-B), the viability of PNTPGS-GN dropped to less than 10%,

while PNPOL-GN at the same concentration (Figure 3-D) had no significant impact on viability (100%, $p < 0.05$).

These viability results suggest that poloxamer 407 may be suitable in situations where a lower cytotoxic effect is desired, such as applications in lesions where cytotoxic effects may lead to irritation or other undesirable outcomes. On the other hand, TPGS exhibited higher cytotoxicity than poloxamer 407 but also induced minimal cell death. Interestingly, TPGS demonstrated a specific cytotoxicity pattern, affecting melanoma cells (Skmel-103) (Figure 3-B) more than normal cells (Figure 3-A), thus both stabilizers have advantages and disadvantages.

Regarding cell uptake (Figure 4), PNTPGS demonstrated a higher percentage than PNPOL, which aligns with expectations based on surface charges that can facilitate nanoparticle internalization. Being a neutral copolymer, poloxamer 407 does not influence the charge balance in the cell membrane. Positively charged nanoparticles are typically internalized via macropinocytosis, while negatively charged nanoparticles are taken up through clathrin-/caveolae-independent endocytosis. Consequently, neutrally charged nanoparticles exhibit lower cellular uptake compared to negatively charged ones. The significant advantage of neutrally charged nanoparticles is their reduced toxicity (Foroozandeh, Aziz, 2018).

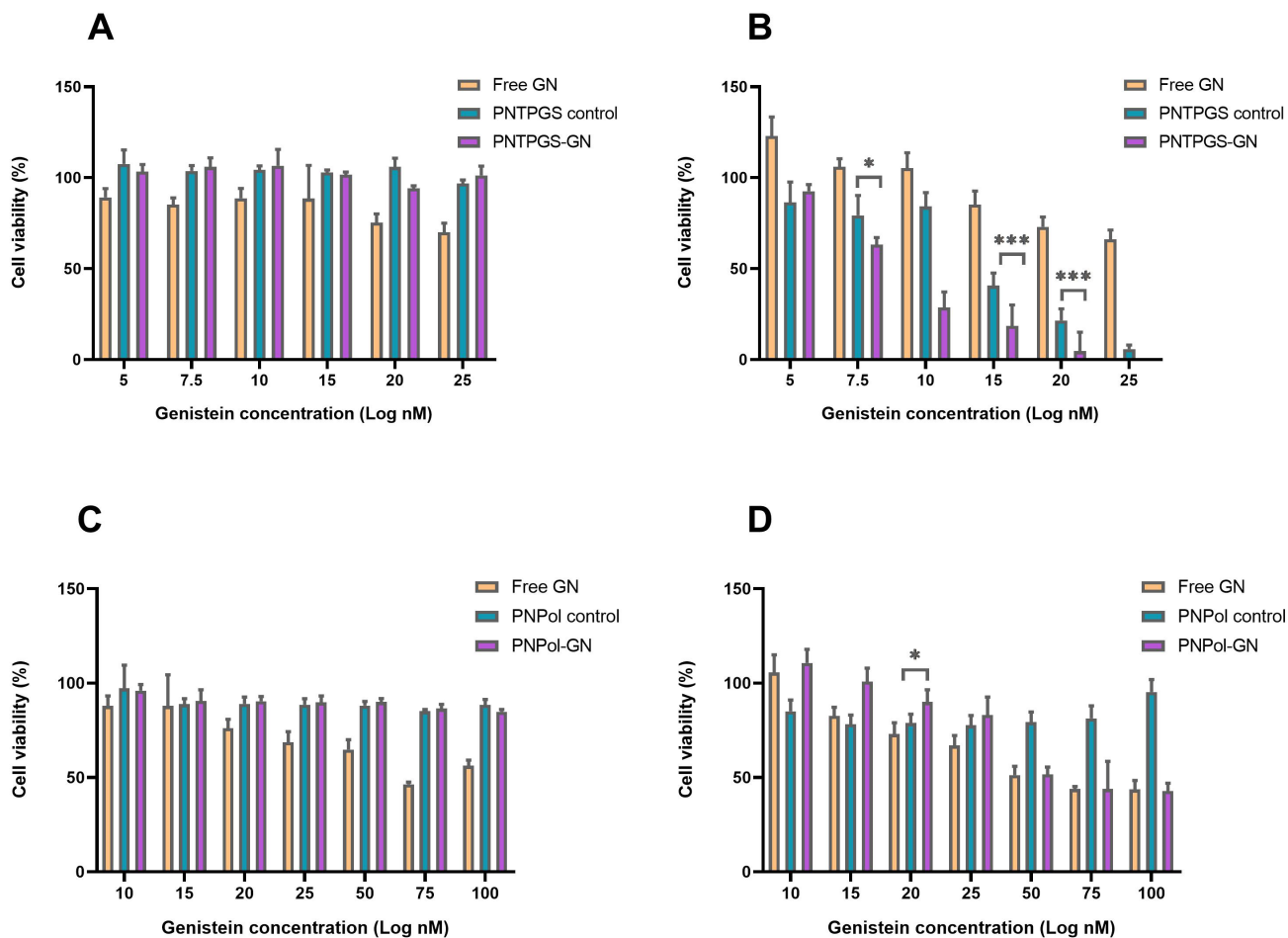


FIGURE 3 – Viability studies of PNTPGS control and containing GN in 3T3 cells (A) and Skmel-103 cells (B) and, PNPoI control and containing GN in 3T3 cells (C) and Skmel-103 cells (D). The viability indicator was resazurin and the results were expressed as average ± S.D, n=6. Statistical analysis was made using Tukey’s test, Two-way ANOVA, 95% of confidence.

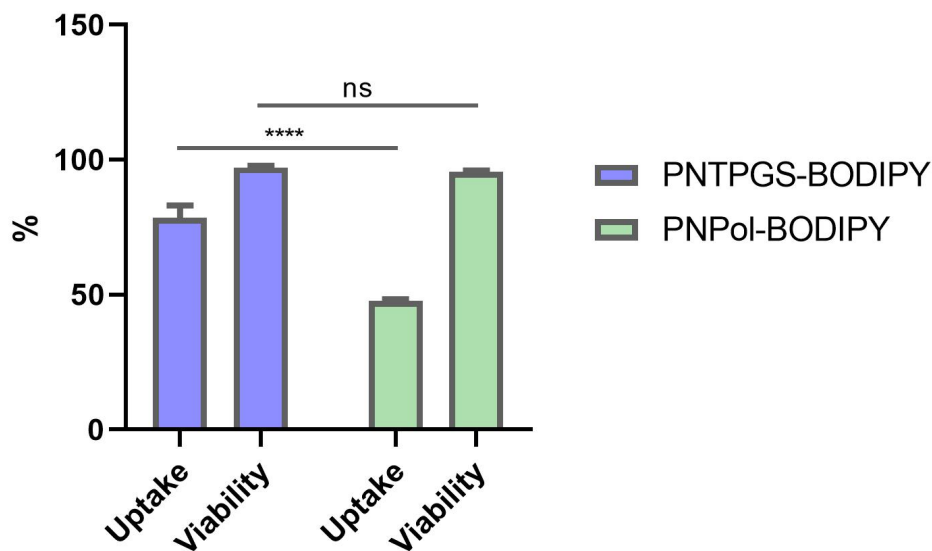


FIGURE 4 – Uptake analysis using Flow Cytometry in which the PCL-based nanoparticles were prepared with PCL bonded with BODIPY. The cell viability was evaluated by propidium iodide. The results were expressed as average ± S.D, n=10. The statistical analysis was made using Tukey’s test, Two-way ANOVA, 95% of confidence. **** p<0.0001.

CONCLUSION

The PCL-based formulations developed, whether with TPGS or poloxamer 407, exhibited particle sizes, PDI, zeta potential, encapsulation efficiency, and GN carrying capacity that make them suitable for evaluation through various administration routes. Additionally, these stabilizers displayed distinct behaviors in cells, with poloxamer showing lower toxicity. However, TPGS demonstrated specificity for tumor cells and a higher uptake percentage. Therefore, this work demonstrates that the choice of stabilizer can offer advantages in different scenarios, considering that both exhibited high GN encapsulation.

ACKNOWLEDGMENTS

The authors would like to extend their gratitude to Jose Orestes Del Ciampo, Henrique Diniz, and Fabiana Rossetto de Moraes from the School of Pharmaceutical Sciences of Ribeirão Preto for their invaluable technical assistance.

FUNDING STATEMENT

This work received support from the São Paulo Research Foundation (FAPESP grant #2017/04091-1), as well as from the Coordenação de Aperfeiçoamento de Pessoal de Nível Superior (CAPES/PROEX 0846/2022 and CAPES Finance Code 001).

CONFLICT OF INTEREST

The authors declare that they have no conflict of interest.

REFERENCES

Abbad S, Abbad S, Waddad AY, Lv H, Zhou J. Preparation, in vitro and in vivo evaluation of Polymeric nanoparticles based on hyaluronic acid-Poly(butyl cyanoacrylate) and D-alpha-tocopheryl Polyethylene glycol 1000 succinate for tumor-targeted delivery of Morin hydrate. *Int J Nanomedicine*. 2015;10:305–20.

Almeida H, Amaral MH, Lobão P, Lobo JMS. Pluronic® F-127 and Pluronic Lecithin Organogel (PLO): main features and

their applications in topical and transdermal administration of drugs. *J Pharm Pharm Sci*. 2012;15(4):592–605.

Averineni RK, Shavi G V, Gurram AK, Deshpande PB, Arumugam K, Maliyakkal N, et al. PLGA 50:50 nanoparticles of paclitaxel: Development, in vitro anti-tumor activity in BT-549 cells and in vivo evaluation. *Bull Mater Sci*. 2012;35(3):319–26.

BRASIL. Ministério da Saúde. RDC nº 166, de julho de 2017. Dispõe sobre a validação de métodos analíticos e dá outras providências. 2017.

De Carvalho Zampieri, Ferreira FS, Resende EC, Gaeti MPN, Diniz DGA, Taveira SF, et al. Biodegradable polymeric nanocapsules based on poly (DL-lactide) for genistein topical delivery: Obtention, characterization and skin permeation studies. *J Biomed Nanotechnol*. 2013;9(3):527–34.

Chorny M, Fishbein I, Danenberg HD, Golomb G. Lipophilic drug loaded nanospheres prepared by nanoprecipitation: effect of formulation variables on size, drug recovery and release kinetics. *J Control Release*. 2002;83(3):389–400.

Crucho CIC, Barros MT. Polymeric nanoparticles: A study on the preparation variables and characterization methods. *Mater Sci Eng C*. 2017;80:771–84.

Cui S, Wang J, Wu Q, Qian J, Yang C, Bo P. Genistein inhibits the growth and regulates the migration and invasion abilities of melanoma cells via the FAK / paxillin and MAPK pathways. *Oncotarget*. 2017;8(13):21674–91.

Da Violante G, Zerrouk N, Richard I, Provot G, Chaumeil JC, Arnaud P. Evaluation of the cytotoxicity effect of dimethyl sulfoxide (DMSO) on Caco2/TC7 colon tumor cell cultures. *Biol Pharm Bull*. 2002;25(12):1600–3.

Danciu C, Soica C, Dehelean C, Zupko I, Csanyi E, Pinzaru I. Preliminary in vitro evaluation of genistein chemopreventive capacity as a result of esterification and cyclodextrin encapsulation. *Anal Cell Pathol*. 2015;2015.

Dobrzynska M, Napierala M, Florek E. Flavonoid nanoparticles: A promising approach for cancer therapy. *Biomolecules*. 2020;10(9):1–17.

Enayati M, Ahmad Z, Stride E, Edirisinghe M. Size mapping of electric field-assisted production of polycaprolactone particles. *J R Soc Interface*. 2010;7(Suppl_4):S393–402.

Farina HG, Pomies M, Alonso DF, Gomez DE. Antitumor and antiangiogenic activity of soy isoflavone genistein in mouse models of melanoma and breast cancer. *Oncol Rep*. 2006;16(4):885–91.

Fessi H, Puisieux F, Devissaguet JP, Ammoury N, Benita S. Nanocapsule formation by interfacial polymer deposition following solvent displacement. *Int J Pharm*. 1989;55(1):R1–4.

- Filipe V, Hawe A, Jiskoot W. Critical evaluation of nanoparticle tracking analysis (NTA) by NanoSight for the measurement of nanoparticles and protein aggregates. *Pharm Res.* 2010;27(5):796–810.
- Foroozandeh P, Aziz AA. Insight into Cellular Uptake and Intracellular Trafficking of Nanoparticles. *Nanoscale Res Lett.* 2018;13.
- Giuliano E, Paolino D, Fresta M, Cosco D. Mucosal applications of poloxamer 407-based hydrogels: An overview. *Pharmaceutics.* 2018a;10(3):1–26.
- Giuliano E, Paolino D, Fresta M, Cosco D. Drug-Loaded Biocompatible Nanocarriers Embedded in Poloxamer 407 Hydrogels as Therapeutic Formulations. *Medicines.* 2018b;6(1):7.
- Goh YX, Jalil J, Lam KW, Husain K, Premakumar CM. Genistein: A Review on its Anti-Inflammatory Properties. *Front Pharmacol.* 2022;13(January):1–23.
- Gross J, Sayle S, Karow AR, Bakowsky U, Garidel P. Nanoparticle tracking analysis of particle size and concentration detection in suspensions of polymer and protein samples: Influence of experimental and data evaluation parameters. *Eur J Pharm Biopharm.* 2016;104:30–41.
- Hewitt A. Soy extract inhibits mammary adenocarcinoma growth in a syngeneic mouse model. *Cancer Lett.* 2003;192(2):133–43.
- ICH. ICH Topic Q2 (R1) Validation of Analytical Procedures: Text and Methodology. *Int Conf Harmon.* 2005;1994(November 1996): 17.
- Ji C, Yang YL, He L, Gu B, Xia JP, Sun WL, et al. Increasing ceramides sensitizes genistein-induced melanoma cell apoptosis and growth inhibition. *Biochem Biophys Res Commun.* 2012;421(3):462–7.
- Kuzumaki T, Kobayashi T, Ishikawa K. Genistein Induces p21Cip1/WAF1 Expression and Blocks the G1 to S Phase Transition in Mouse Fibroblast and Melanoma Cells. *Biochem Biophys Res Commun.* 1998;251(1):291–5.
- Legrand P, Lesieur S, Bochot A, Gref R, Raatjes W, Barratt G, et al. Influence of polymer behaviour in organic solution on the production of polylactide nanoparticles by nanoprecipitation. *Int J Pharm.* 2007;344(1–2):33–43.
- Li C, Wallace S. Polymer-drug conjugates: Recent development in clinical oncology. *Adv Drug Deliv Rev.* 2008;60(February):886–98.
- Mainardes RM, Evangelista RC. PLGA nanoparticles containing praziquantel: Effect of formulation variables on size distribution. *Int J Pharm.* 2005;290(1–2):137–44.
- Mora-Huertas CE, Garrigues O, Fessi H, Elaissari A. Nanocapsules prepared via nanoprecipitation and emulsification-diffusion methods: Comparative study. *Eur J Pharm Biopharm.* 2012;80(1):235–9.
- Nordström P. Formation of polymeric nanoparticles encapsulating and releasing a new hydrophobic cancer drug. [Tese Formation of polymeric nanoparticles encapsulating and releasing a new hydrophobic cancer drug]. Chalmers University of Technology; 2011.
- Pavese JM, Farmer RL, Bergan RC. Inhibition of cancer cell invasion and metastasis by genistein. *Cancer Metastasis Rev.* 2010;29(3):465–82.
- Pool H, Campos-Vega R, Herrera-Hernández MG, García-Solis P, García-Gasca T, Sánchez IC, et al. Development of genistein-PEGylated silica hybrid nanomaterials with enhanced antioxidant and antiproliferative properties on HT29 human colon cancer cells. *Am J Transl Res.* 2018;10(8):2306–23.
- Rauth S, Kichina J, Green A. Inhibition of growth and induction of differentiation of metastatic melanoma cells in vitro by genistein: Chemosensitivity is regulated by cellular p53. *Br J Cancer.* 1997;75(11):1559–66.
- Sharifi-Rad J, Quispe C, Imran M, Rauf A, Nadeem M, Gondal TA, et al. Genistein: An Integrative Overview of Its Mode of Action, Pharmacological Properties, and Health Benefits. *Oxid Med Cell Longev.* 2021;2021(June).
- Singh P, Sharma S, Rath SK. Genistein induces deleterious effects during its acute exposure in Swiss mice. *Biomed Res Int.* 2014;619617.
- Tyagi N, Song YH, De R. Recent progress on biocompatible nanocarrier-based genistein delivery systems in cancer therapy. *J Drug Target.* 2019;27(4):394–407.
- Venza I, Visalli M, Oteri R, Beninati C, Teti D, Venza M. Genistein reduces proliferation of EP3-expressing melanoma cells through inhibition of PGE2-induced IL-8 expression. *Int Immunopharmacol.* 2018;62(May):86–95.
- Yan A, Bussche A von Dem, Kane AB, Hurt RH. Tocopheryl Polyethylene Glycol Succinate as a Safe, Antioxidant Surfactant for Processing Carbon Nanotubes and Fullerenes. *Carbon N Y.* 2007;45:2463–70.
- Zhang H, Liu G, Zeng X, Wu Y, Yang C, Mei L, et al. Fabrication of genistein-loaded biodegradable TPGS-b-PCL nanoparticles for improved therapeutic effects in cervical cancer cells. *Int J Nanomed.* 2015;10:2461–73.

Received for publication on July 12th, 2022.

Accepted for publication on December 05th, 2022.